Structural and bonding properties of bcc-based B_{80} solids

Amy Y. Liu,[1,2] Rajendra R. Zope,[3] and Mark R. Pederson[2]
[1]*Department of Physics, Georgetown University, Washington, DC 20057, USA*
[2]*Center for Computational Materials Science, Naval Research Laboratory, Washington, DC 20375, USA*
[3]*Department of Physics, University of Texas at El Paso, El Paso, Texas 79958, USA*
(Received 30 June 2008; revised manuscript received 7 September 2008; published 16 October 2008)

A density-functional-theory investigation of bcc B_{80} and K_6B_{80} is presented. The calculations show that B_{80} cages pack closely on a bcc lattice, with bond formation between atoms on both nearest-neighbor and next-nearest-neighbor molecules. While the binding energy of 9.9 eV/molecule is only about half that calculated for fcc B_{80}, potassium intercalation of bcc B_{80} adds an ionic component to the binding to further stabilize the lattice. Both B_{80} and K_6B_{80} are calculated to be metallic. The electronic structure is analyzed in terms of ionic and covalent effects, and the bonding is discussed in terms of a balance between two- and three-center bonding.

DOI: 10.1103/PhysRevB.78.155422 PACS number(s): 81.05.Tp, 61.50.Lt, 71.20.Tx

I. INTRODUCTION

Molecular solids based on C_{60} fullerenes exhibit a broad range of electronic properties.[1,2] Crystal structure, orientational ordering, dimensionality, and doping can tune the balance between competing interactions, such as the intramolecular Coulomb repulsion and the intermolecular hopping. This leads to a rich phase diagram with a variety of observed electronic ground states, including correlated insulators, semiconductors, metals, superconductors,[3,4] and soft ferromagnets.[5] Pure C_{60} molecules, for example, condense into an fcc solid weakly bound by the van der Waals interaction. The electronic structure maintains its molecular character, and the solid is a band insulator. Upon intercalation by alkali atoms, the fullerene molecules accept electrons from the intercalants, and the binding is almost entirely ionic.[6,7] The fcc-based A_3C_{60} compounds, with A=K or Rb, are metallic, as expected from band theory, and become superconducting at low temperatures. Band-structure calculations indicate that the body-centered tetragonal (bct) A_4C_{60} material should also be metallic. However, experiments find it to be an insulator, suggesting the importance of correlations.[8] The fully intercalated material, bcc A_6C_{60}, is insulating, consistent with band theory. Larger intercalants such as Cs are difficult to accommodate in the fcc lattice, and an alternative structure for Cs_3C_{60} has been identified as the bcc-based A15 structure.[9] At ambient pressure, A15 Cs_3C_{60} is believed to be a Mott insulator, but upon compression, it metalizes and becomes superconducting.

Hollow fullerenelike structures have been proposed for boron clusters,[10] and recent first-principles calculations have predicted an energetically favorable icosahedral cage structure for B_{80}, analogous to C_{60}.[11,12] The B_{80} structure can be built from the C_{60} structure, which has 12 pentagonal rings and 20 hexagonal rings, by adding an atom at the center of each hexagonal ring. The energetic stability of this structure can be understood in terms of a balance between the number of pentagons, which are electron deficient, and the number of capped hexagons, which are electron rich.[13] A natural question is whether solid phases of pure and intercalated B_{80} are possible, and how their properties would compare to those of the fullerides. While the B_{80} and C_{60} cages are isoelectronic and structurally similar, the chemistry of boron and that of carbon are very different, which could lead to fundamental differences in the solid state.

Yan *et al.*[14] recently reported density-functional-theory (DFT) calculations for fcc B_{80}, finding it to be more stable than isolated B_{80} by 0.23 eV/atom. The molecules are significantly distorted in this solid to allow four bonds to form between each pair of neighboring B_{80} cages. We have independently discovered the same results.[15] In this paper we explore the structural and electronic properties of bcc-based B_{80} solids, both the pure material and potassium-intercalated K_6B_{80}. The bcc structure is conducive to the formation of intermolecular bonds between B atoms on (111) facets (i.e., capped hexagons) which makes it different from both fcc B_{80} and bcc C_{60} solids. Although our DFT calculations show that the bcc solid is not as strongly bound as the fcc solid, potassium intercalation adds an ionic contribution to the binding energy to further stabilize the bcc lattice. Due to the enhanced intermolecular interactions (compared to fullerides), there are significant shifts and broadening of electronic bands, leading to dispersive bands with little resemblance to the molecular spectrum. The electronic structure and bonding are analyzed in terms of effects from ionic bonding and intermolecular covalent bond formation. While the strong intermolecular interactions likely reduce electron correlation effects that give rise to interesting behavior in C_{60} solids, they also reveal a versatility in boron's ability to bond in different configurations.

II. COMPUTATIONAL METHOD

Structural energetics and electronic structure are determined within density-functional theory as implemented within the PWSCF code.[16] The interaction between electrons and ionic cores is described by ultrasoft pseudopotentials.[17] Nonlinear core corrections are used to treat the overlap between core and valence charge densities in B,[18] while the K 3*s* and 3*p* semicore states are included as valence states. The exchange-correlation interaction is treated with the local-density approximation (LDA) using the Perdew-Zunger parametrization[19] of the correlation energy. Tests employing the generalized gradient approximation yield qualitatively

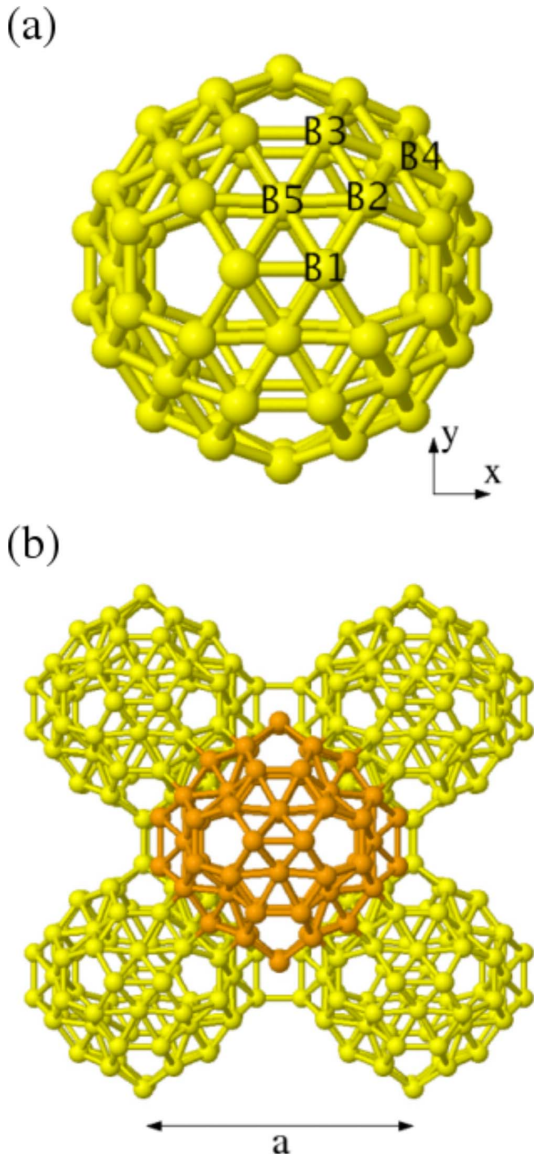

FIG. 1. (Color online) (a) Isolated B_{80} cluster with T_h symmetry. The five inequivalent sites are labeled. Cartesian axes are chosen to be parallel to B1-B1 dimers that are shared by two hexagons. The [111] directions correspond to threefold axes on which the B4 sites lie. (b) Optimized geometry for bcc B_{80}. The orientation of the Cartesian axes is the same as in (a). The four clusters with light gray (yellow) atoms occupy corners on the base of the cube ($z=0$), while the central darker cluster (orange) occupies the body-center site in the next lattice plane ($z=a_0/2$). Intercluster bonds connect (111) faces of neighboring clusters, as well as B1 atoms on next-nearest neighbors.

similar results for structural properties and energetics but smaller intermolecular binding energies. One-electron wave functions are expanded in a plane-wave basis set with a kinetic-energy cutoff of 30 Ry. The Brillouin zone is sampled on a uniform mesh of $2\times2\times2$ **k** points, which is sufficient for total-energy convergence of 1 meV/atom. For fixed lattice constants, ionic positions are relaxed from several starting configurations until all force components are less than 10^{-3} Ry/a.u.

TABLE I. Boron-boron bond lengths in bcc B_{80} and K_6B_{80}. Bond lengths are given in Å. There are two inequivalent bonds joining B2 and B3 sites: one is shared by two hexagons (hh) and one is shared by a pentagon and a hexagon (ph).

	B_{80}	B_{80}	B_{80}	$B_{80}K_6$
a (Å)	20.00	12.32	10.93	12.32
		Intracluster		
B1-B1	1.67	1.69	1.87	1.70
B1-B2	1.71	1.70	1.79	1.70
B1-B5	1.69	1.70	1.78	1.74
B2-B3(hh)	1.66	1.68	1.70	1.66
B2-B3(ph)	1.71	1.70	1.72	1.71
B2-B4	1.69	1.81	1.81	1.82
B2-B5	1.69	1.68	1.74	1.69
B3-B3	1.71	1.68	1.67	1.69
B3-B4	1.69	1.81	1.75	1.81
B3-B5	1.69	1.68	1.77	1.68
		Intercluster		
B1-B1			1.82	
B2-B3			1.87	
B4-B4		1.72		1.70

III. RESULTS AND DISCUSSION

A. Structural properties

Although isolated B_{80} was originally proposed to have the same icosahedral point-group symmetry (I_h) as C_{60},[11] it has been shown that icosahedral B_{80} is vibrationally unstable and that an unconstrained relaxation leads to a vibrationally stable B_{80} cluster with T_h symmetry.[20,21] The T_h cluster has five inequivalent sites, which are labeled in Fig. 1(a): 12 B1 sites on hexagon-hexagon bonds parallel to the Cartesian directions, 24 B2 and 24 B3 sites on other edges that adjoin two hexagons, 8 B4 hexagon-capping sites along [111] and equivalent directions, and 12 B5 sites capping the remaining hexagons. The equivalence of the 20 hexagon-capping sites in I_h symmetry is broken, but in the isolated molecule both sets of capped hexagons are relatively flat, with just a slight inward puckering of the center site.

Unless otherwise indicated, for a bcc lattice of B_{80} clusters, we assume that every cluster is oriented as shown in Fig. 1 with cubic crystallographic axes aligned with the Cartesian directions. As T_h is a subgroup of the full cubic group, the structural relaxations of the solid are constrained to maintain T_h symmetry. Since the energy landscape is complicated, with multiple basins of attraction, ionic positions are optimized using several starting configurations for each lattice constant.[22]

At $a=20$ Å, the shortest distance between atoms on one cluster and those on a neighboring one is over 9.6 Å, compared with about 1.7 Å for intracluster bond lengths (Table I). In this paper, we use the $a=20$ Å results as an approximation for isolated clusters. For lattice constants between about 15 and 20 Å, the intercluster interactions are weak,

and the cluster geometry varies little with lattice spacing. Below about 15 Å, the distortion of the clusters starts to become more evident. For a small range of lattice constants, between about 11.8 and 12.8 Å, the lowest energy configuration corresponds to a separate minimum, in which, rather than puckering inward, the eight B4 atoms pucker outward along the body diagonal directions to form two-centered bonds with counterparts on neighboring molecules. As seen in Table I, at $a=12.32$ Å, the intracluster bonds that do not involve B4 sites are close to the lengths of those in the isolated molecule. The significant outward puckering of B4 sites along the [111] directions stretches the intracluster B2-B4 and B3-B4 distances. At the same time, the distance between B4 sites on neighboring clusters is reduced to a value within the range spanned by intracluster bonds.

As the lattice constant is decreased further, the structure with outward puckering of the (111) facets relaxes without a barrier to a configuration in which the capped hexagons pucker inward. This allows the six B atoms on the edge of the (111) facet (of types B2 and B3) to bond weakly with their counterparts on the neighboring clusters. At the same time the cages pucker outward along the Cartesian directions. At the optimized lattice constant of $a=10.93$ Å, the shortest intercluster distance is actually between B1 atoms on *second-nearest-neighbor* clusters (Table I). The intercluster bonds between nearest and second-nearest neighbors can be seen in Fig. 1(b). The geometry of the bonds between next-nearest neighbors resembles what is observed in some polymerized C_{60} materials, in which the [2+2] cycloaddition mechanism converts two hexagon-hexagon bonds on adjacent molecules into a fourfold ring.[23] In bcc B_{80}, the intramolecular B1-B1 dimers that form two of the sides of each fourfold ring are significantly weakened, as indicated by their elongation to 1.87 Å.

The calculated LDA binding energy of bcc B_{80} relative to an isolated B_{80} molecule is 9.9 eV/molecule. This is just over half the value for fcc B_{80}.[14,15] Both fcc and bcc B_{80} lie above the rhombohedral α polymorph of solid boron, by 0.35 and 0.46 eV/atom, respectively. In both the fcc and bcc B_{80} solids, the boron cage is significantly distorted. In fcc B_{80}, each molecule forms four strong bonds (of types B1-B5 and B3-B3) with each of its 12 neighboring molecules, while in bcc B_{80}, each molecule forms two covalent B1-B1 bonds with each of its six second neighbors and six weaker bonds with each of its eight nearest neighbors.

To check the dependence of the intercluster bonding on cluster orientation, we have considered several randomly chosen orientations for the B_{80} molecule on the bcc lattice, all of which reduce the symmetry below T_h. In all cases, strong intermolecular bonds form, accompanied by significant distortions of the B_{80} cages. The energies of the various orientations tested are within a few tenths of an eV per molecule of the original T_h orientation, so the fcc solid remains significantly more favorable than these bcc-based structures. On the other hand, preliminary results suggest that a CsCl-like structure in which the molecules on different simple-cubic sublattices of the bcc lattice are rotated 90° with respect to each other could be competitive with the fcc solid.

All the B_{80} solids are calculated to be much more strongly bound than solid C_{60}, for which the LDA gives a binding energy of 1–1.6 eV/molecule,[7,24] close to the experimentally determined heat of sublimation.[25] Although covalently bonded three-dimensional C_{60} polymer networks have been synthesized under high-temperature and high-pressure conditions, they differ from the predicted B_{80} solids in that the binding energies of the dense C_{60} solids are less than that of the fcc van der Waals solid.[26]

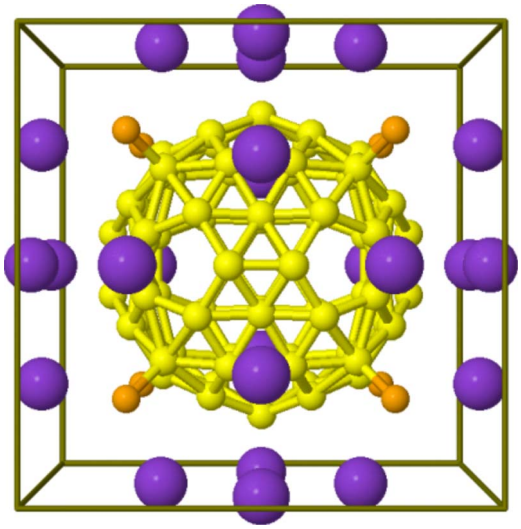

FIG. 2. (Color online) Structure of bcc-based K_6B_{80}. The box indicates the cubic cell with sides $a_0=12.32$ Å. The borons on the molecule occupying the body-centered site are light gray (yellow). The large dark spheres (purple) are the surrounding potassium atoms. The B4 borons pucker outward to form bonds with B4 borons, shown as small medium gray (orange) spheres, on molecules occupying the corner sites of the cube. For clarity, only a single boron (medium gray or orange) from each corner-occupying B_{80} is shown.

When C_{60} is intercalated to saturation with potassium, it condenses into a bcc lattice with six potassium atoms per C_{60}.[2] We examine the properties of the analogous bcc-based K_6B_{80} as an example of an alkali-intercalated B_{80} solid. The point group of the crystal structure is T_h. The B_{80} situated at the center of the cube is surrounded by a cage of 24 K atoms on the six faces of the cube. The four K atoms on each face form a rhombus, where two of the K atoms face capped hexagons and two face pentagons on the central B_{80}, as shown in Fig. 2. The long diagonal of the rhombus has length $2a\delta$, while the short diagonal has length $2a(0.5-\delta)$. For a square, in which each K atom occupies a tetrahedral interstitial site of the bcc lattice, the dimerization parameter δ is 0.25. When $\delta>(<).25$, the long (short) diagonal of the rhombus is parallel to the B1-B1 dimers shared by adjoining hexagons.

Intercalation increases the optimal lattice constant to $a_0=12.32$ Å in K_6B_{80}. This suppresses the formation of intercluster B1 fourfold rings. Instead, covalent intercluster bonding occurs between outward-puckered B4 atoms, as shown in Fig. 2. The positions of the boron atoms are very similar to their positions in pure bcc B_{80} at the same lattice constant. The main structural difference is a stronger inward puckering of the B5 hexagon-capping sites induced by the intercalant. The structural similarity between the pure and intercalated systems is reflected in the bond lengths listed in Table I.

Energetically, K_6B_{80} is more stable than phase separated bcc K and bcc B_{80} by 10.5 eV/f.u. Relative to bcc K and fcc B_{80}, it is 0.8 eV/f.u. lower in energy.

The distortion of the K rhombus is characterized by a dimerization coordinate of $\delta=0.273$, which is close to the calculated and measured values in K_6C_{60}.[2,27] Unlike in the fulleride though, the shortest B-K distance is not between a pentagon-facing K and B1 boron (3.21 Å) but rather between a hexagonal-facing K and a B5 hexagon-capping boron (3.16 Å). The hexagonal-facing K is also close (3.22 Å) to two B3 sites next to the nearest-neighbor B5 site. The proximity of each K to multiple B sites differs from the situation in C_{60} and could enhance the ionic binding.

Boustani[28] postulated an Aufbau principle for constructing highly stable boron clusters, surfaces, and networks. The general idea is that such structures can be generated from the two basic motifs of pentagonal and hexagonal pyramids. The (111) faces of isolated B_{80} follow the Aufbau principle, though the puckering of the hexagonal pyramids is unusually weak. In the bcc solids, the enhanced puckering of the (111) faces and the accompanying formation of intermolecular bonds mirror the motifs found in buckled double-layer boron clusters that have been predicted to be highly stable.[29] It is also reminiscent of the stuffed fullerenelike boron clusters with a central B_{12} icosahedron that have recently been calculated to be more stable than hollow counterparts.[30] If viewed as two nested cages, boron atoms in triangular regions on the outer cage pucker inward to form σ bonds with those in the inner icosahedron. Thus despite the relatively low energy of the isolated B_{80} cage among hollow spherical structures,[12] results for the solids and the nested boron cages indicate a preference to form buckled surfaces that allow intermolecular covalent bonding, which is in clear distinction to carbon analogs. Calculations on bundled boron nanotubes have revealed a similar propensity.[31]

B. Electronic structure and bonding

Both bcc B_{80} and K_6B_{80} are calculated to be metallic. Because of the strong intermolecular bonding, the band structure in the solid state differs substantially from the spectrum of molecular states.

The densities of states (DOSs) for bcc B_{80} with lattice constants of 20, 12.32, and 10.93 Å are shown in the top three panels of Fig. 3. In panel (a), the nearly discrete spectrum is broadened by 0.005 Ry, while a larger broadening parameter of 0.01 Ry is used for the metallic DOS in the remaining panels. In the isolated molecule with T_h symmetry, the twofold-degenerate highest occupied molecular orbital (HOMO) belongs to the e_u representation while the threefold degenerate lowest unoccupied molecular orbital (LUMO) has t_u symmetry. Both HOMO and LUMO states are derived mainly from out-of-plane p orbitals, and they are separated by an energy gap of about 1 eV. The HOMO charge is concentrated on the B2 and B3 sites, while the LUMO charge populates the B1, B2, and B3 sites.[21] At $a=12.32$ Å, with relaxed internal coordinates, the DOS still retains some features that are present in the molecular spectrum, such as the large peak about 2 eV below the Fermi level. This peak

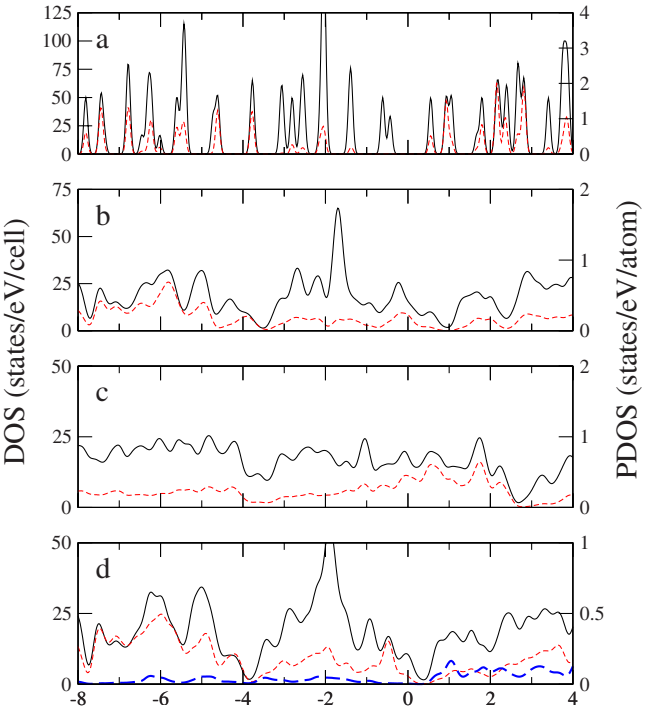

FIG. 3. (Color online) Electronic density of states of (a) bcc B_{80} with $a=20$ Å, (b) bcc B_{80} with $a=12.32$ Å, (c) bcc B_{80} with $a=10.93$ Å, and (d) K_6B_{80} with $a=12.32$ Å. The zero of energy corresponds to the Fermi level. The projected densities of states for B4 atoms and K atoms are plotted with thin dashed (red) and thick dashed (blue) lines, respectively. Note that different scales are used for the total and projected densities of states.

arises mainly from in-plane orbitals on B1, B2, and B3 sites (i.e., in-plane bonds around hexagonal and pentagonal rings). An examination of the bands reveals that the LUMO and HOMO manifolds broaden and overlap with each other, filling in the gap. Furthermore, the puckering and bond formation between B4 sites on neighboring molecules split the states with significant weight on B4 sites, which originally lie above the Fermi level. Some states with bonding character drop below the Fermi level, as can be seen in the B4 projected density of states (PDOS). At the optimized lattice constant of $a_0=10.93$ Å, the cage structure is significantly distorted, and the resulting bands and DOS have little resemblance to either the molecular spectrum or the $a=12.32$ Å bands. In particular, since the intercluster bonding to both the nearest and second-nearest neighbors disrupts the in-plane intramolecular bonds, the peak about 2 eV below the Fermi level is gone. Several bands cross the Fermi level, with bandwidths of 0.5–1 eV, and the DOS near the Fermi level has contributions from all the B sites.

Figure 3(d) shows the DOS of optimized K_6B_{80}. With a lattice constant of 12.32 Å, features in the DOS corresponding to those of undoped B_{80} at the same lattice constant are evident, reflecting the structural similarities of the boron cages. States with K 4s character are found above the Fermi level, indicating significant charge transfer from the alkali atoms to the B_{80} clusters. In fact, the Löwdin charges indicate a nearly complete ionization of the alkali atoms (Table II). As in panel (b), B4 intermolecular bonding states are

TABLE II. Löwdin valence charges for bcc B_{80} and K_6B_{80}.

	B_{80}	B_{80}	B_{80}	K_6B_{80}
a (Å)	20	12.32	10.93	12.32
B1	3.02	3.01	3.06	3.15
B2	3.01	2.99	2.98	3.09
B3	3.01	3.00	3.05	3.08
B4	2.76	2.91	2.80	2.92
B5	2.75	2.79	2.82	2.78
K				0.10

found below the Fermi level. By analogy with K_6C_{60}, one might have expected K_6B_{80} to be semiconducting, with the six electrons donated to the cluster by the alkali atoms filling the three-band manifold derived from the molecular LUMO. But with the significant broadening and overlap of the HOMO and LUMO and the shift of B4 bonding states to below the Fermi level, the rigid-band picture that worked reasonably well for K_6C_{60} completely fails.

While care should be taken not to overinterpret the values of the Löwdin charges listed in Table II, some trends are evident. For the nearly isolated molecule, the charge population is smaller on the hexagon-capping sites (B4 and B5) than on other sites. In K_6B_{80}, the B4 site recovers charge, but the B5 site does not. In addition, the charge donated from K resides mainly on B1, B2, and B3 sites. These trends can be understood in terms of the balance between two-center and three-center bonding as discussed by Tang and Ismail-Beigi[13] in the context of boron sheets. In terms of optimizing stability, boron in a honeycomb lattice with two-center sp^2 bonds is electron deficient. On the other hand, triangular sheets of boron with three-center two-electron bonds would prefer to donate electrons to minimize occupation of antibonding in-plane orbitals. The relatively large cohesive energy of the B_{80} cluster arises from the balance between filled flat hexagons which are electron rich and open pentagons which are electron poor. The Löwdin charges indicate that the flat hexagon-capping sites in isolated B_{80} indeed give up some charge to other regions of the cluster. However, once the B4 capping sites on the (111) hexagons become puckered to form intermolecular bonds, it becomes more favorable for the B4 sites to retain their charge to populate intermolecular bonding states. The other hexagon-capping sites (B5) continue to donate charge since they remain relatively flat and do not participate in intermolecular bonding. Upon K doping, the electron-poor regions of the cluster accept most of the donated electrons.

In their investigation of fcc B_{80}, Yan *et al.*[14] noted some qualitative similarities in the electronic DOS compared to the two-band layered superconductor MgB_2. One crucial factor in the superconductivity of layered borides is the balance between σ, π, and interlayer states at the Fermi level.[32] Although the σ states provide the largest contribution to coupling to phonons in MgB_2, the π states play a crucial but indirect role in screening the in-plane vibrational modes. In the B_{80} solids, there is the possibility of tuning the occupation of σ and π states through structure and intercalation, but a detailed analysis of the character of the bands and their coupling to vibrational states would be needed to assess the potential for superconductivity in these materials.

IV. CONCLUSIONS

Density functional calculations indicate that, like C_{60}, spherical cagelike B_{80} molecules can condense into stable solids. In both fcc and bcc B_{80}, covalent bonds form between molecules, so that the binding energies of the B_{80} solids are much larger than that of solid C_{60}. While B_{80} is less stable in the bcc lattice than in the fcc structure, the stability of the bcc lattice can be enhanced through intercalation with potassium. The binding of K_6B_{80} has significant ionic and covalent contributions. In contrast to C_{60} fullerides, the strong intermolecular interactions in B_{80} solids are expected to suppress strong correlation effects, making it perhaps less interesting in terms of being able to tune between a variety of fundamentally different electronic ground states. On the other hand, just among the fcc, bcc, and doped bcc solids, many different intermolecular bonding configurations have been found, indicating an unusual chemical versatility. In comparison to existing forms of crystalline boron, which are all semiconducting and based on the B_{12} icosahedral unit, all of the B_{80}-based solids considered thus far are conducting. It would be interesting to explore the coupling of electronic and vibrational states in various forms of pure and intercalated B_{80}, as there could be similarities to layered boride superconductors.

ACKNOWLEDGMENTS

This work was supported by the National Science Foundation through Grant No. DMR-0705266 and through TeraGrid resources at TACC and NCSA.

[1] O. Gunnarsson, *Alkali-Doped Fullerides: Narrow Band Solids with Unusual Properties* (World Scientific, Singapore, 2004).
[2] O. Zhou and D. E. Cox, J. Phys. Chem. Solids **53**, 1373 (1992).
[3] A. F. Hebard, M. J. Rosseinsky, R. C. Haddon, D. W. Murphy, S. H. Glarum, T. T. M. Palstra, A. P. Ramirez, and A. R. Kortan, Nature (London) **350**, 600 (1991); K. Tanigaki, T. W. Ebbesen, S. Saito, J. Mizuki, J. S. Tsai, Y. Kubo, and S. Kuroshima, *ibid.* **352**, 222 (1991).
[4] O. Gunnarsson, Rev. Mod. Phys. **69**, 575 (1997).
[5] P. M. Allemand, K. C. Khemani, A. Koch, F. Wudl, K. Holczer, S. Donovan, G. Gruner, and J. D. Thompson, Science **253**, 301 (1991).
[6] S. C. Erwin and M. R. Pederson, Phys. Rev. Lett. **67**, 1610 (1991).

[7] S. Saito and A. Oshiyama, Phys. Rev. B **44**, 11536 (1991); J. L. Martins and N. Troullier, *ibid.* **46**, 1766 (1992).
[8] R. F. Kiefl, T. L. Duty, J. W. Schneider, A. MacFarlane, K. Chow, J. W. Elzey, P. Mendels, G. D. Morris, J. H. Brewer, E. J. Ansaldo, C. Niedermayer, D. R. Noakes, C. E. Stronach, B. Hitti, and J. E. Fischer, Phys. Rev. Lett. **69**, 2005 (1992); D. W. Murphy, M. J. Rosseinsky, R. M. Fleming, R. Tycko, A. P. Ramirez, R. C. Haddon, T. Siegrist, G. Dabbagh, J. C. Tully, and R. E. Walstedt, J. Phys. Chem. Solids **53**, 1321 (1992).
[9] A. Y. Ganin, Y. Takabayashi, Y. Z. Khimyak, S. Margadonna, A. Tamai, M. J. Rosseinsky, and K. Prassides, Nature Mater. **7**, 367 (2008).
[10] I. Boustani, J. Solid State Chem. **133**, 182 (1997).
[11] N. Gonzalez Szwacki, A. Sadrzadeh, and B. I. Yakobson, Phys. Rev. Lett. **98**, 166804 (2007).
[12] N. Gonzalez Szwacki, Nanoscale Res. Lett. **3**, 49 (2008).
[13] H. Tang and S. Ismail-Beigi, Phys. Rev. Lett. **99**, 115501 (2007).
[14] Q.-B. Yan, Q.-R. Zheng, and G. Su, Phys. Rev. B **77**, 224106 (2008).
[15] A. Y. Liu (unpublished).
[16] http://www.pwscf.org
[17] D. Vanderbilt, Phys. Rev. B **41**, 7892 (1990).
[18] S. G. Louie, S. Froyen, and M. L. Cohen, Phys. Rev. B **26**, 1738 (1982).
[19] J. P. Perdew and A. Zunger, Phys. Rev. B **23**, 5048 (1981).
[20] G. Gopakumar, M. T. Nguyen, and A. Ceulemans, Chem. Phys. Lett. **450**, 175 (2008).
[21] T. Baruah, M. R. Pederson, and R. R. Zope, Phys. Rev. B **78**, 045408 (2008).
[22] Lattice constants were sampled in steps of 0.5 Å, from $a = 10.5-15$ Å, using two starting configurations: the isolated B_{80} coordinates and isolated B_{80} with outward-puckered B4 sites. Then, any relaxed structure that deviated qualitatively from the starting structure was tested as a starting point for other lattice constants. A more dense sampling of lattice constants was used to explore the minimum and regions with competitive phases.
[23] A. M. Rao, P. Zhou, K.-A. Wang, G. T. Hager, J. M. Holden, Y. Wang, W.-T. Lee, X.-X. Bi, P. C. Eklund, D. S. Cornett, M. A. Duncan, and I. J. Amster, Science **259**, 955 (1993); P. Zhou, Z.-H. Dong, A. M. Rao, and P. C. Eklund, Chem. Phys. Lett. **211**, 337 (1993); C. Goze, F. Rachdi, L. Hajji, M. Nunez-Regueiro, L. Marques, J.-L. Hodeau, and M. Mehring, Phys. Rev. B **54**, R3676 (1996).
[24] M. Hasegawa, N. Nishidate, M. Katayama, and T. Inaoka, J. Chem. Phys. **119**, 1386 (2003).
[25] C. Pan, M. P. Sampson, Y. Chai, R. H. Hauge, and J. L. Margrave, J. Phys. Chem. **95**, 2944 (1991).
[26] S. Yamanaka, A. Kubo, K. Inumaru, K. Komaguchi, N. S. Kini, T. Inoue, and T. Irifune, Phys. Rev. Lett. **96**, 076602 (2006); S. Yamanaka, N. S. Kini, A. Kubo, S. Jida, and H. Kuramoto, J. Am. Chem. Soc. **130**, 4303 (2008).
[27] M. R. Pederson, S. C. Erwin, W. E. Pickett, K. A. Jackson, and L. L. Boyer, in *Physics and Chemistry of Finite Systems: From Clusters to Crystals*, edited by P. Jena, S. N. Khanna, and B. K. Rao (Kluwer, Dordrecht, 1992), Vol. II, p. 1323.
[28] I. Boustani, Phys. Rev. B **55**, 16426 (1997).
[29] I. Boustani, Surf. Sci. **370**, 355 (1997).
[30] D. L. V. K. Prasad and E. D. Jemmis, Phys. Rev. Lett. **100**, 165504 (2008).
[31] J. Kunstmann and A. Quandt, Chem. Phys. Lett. **402**, 21 (2005).
[32] A. Y. Liu and I. I. Mazin, Phys. Rev. B **75**, 064510 (2007).